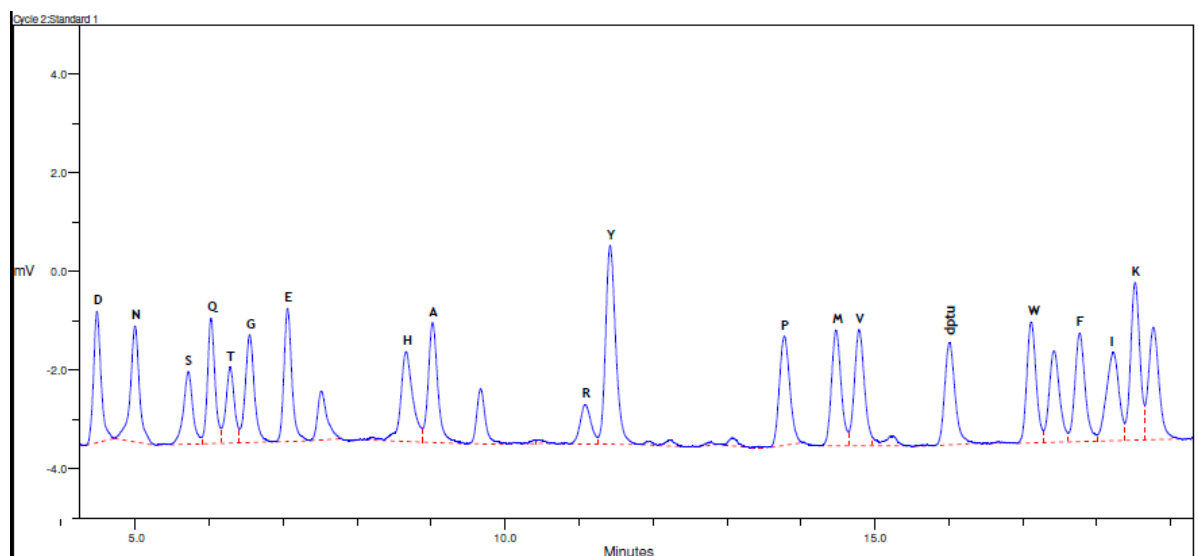
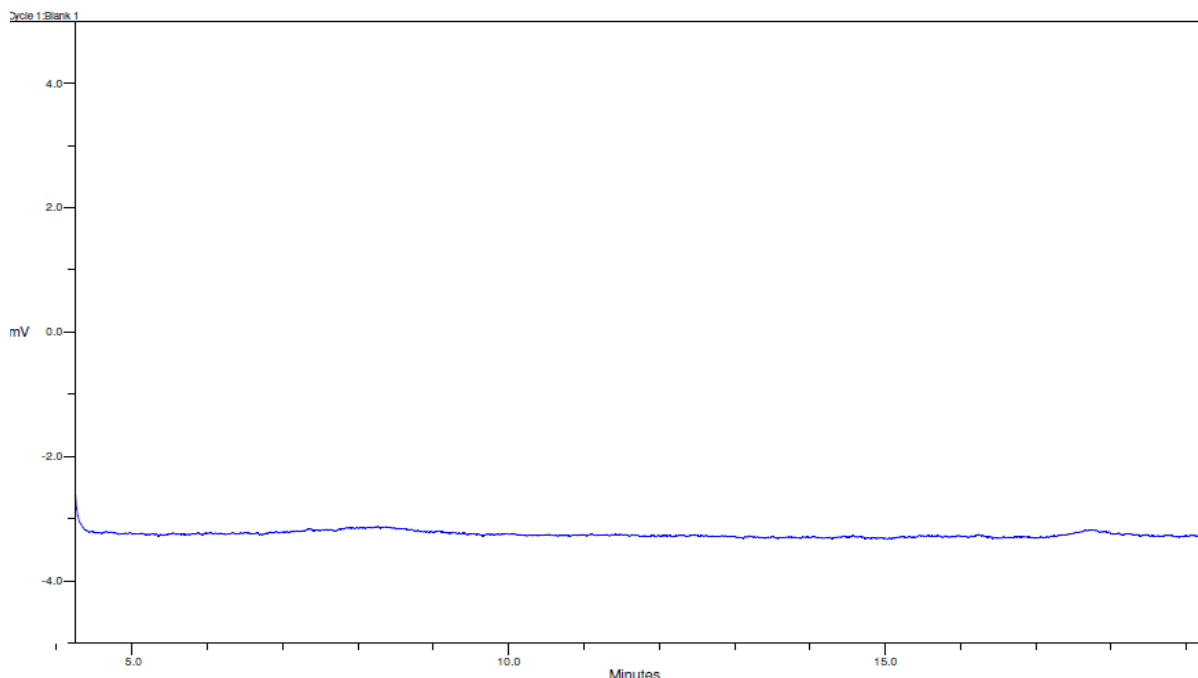
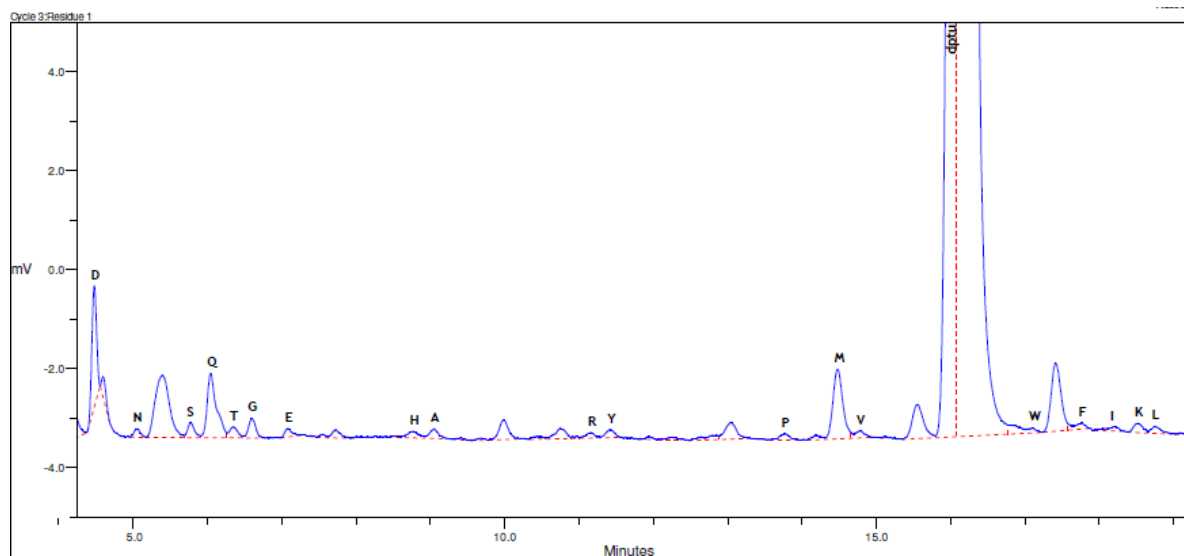


Supplementary Materials: A Novel Method of Affinity Tag Cleavage in Purification of a Recombinant Thermostable Lipase from *Aneurinibacillus thermoaerophilus* strain HZ

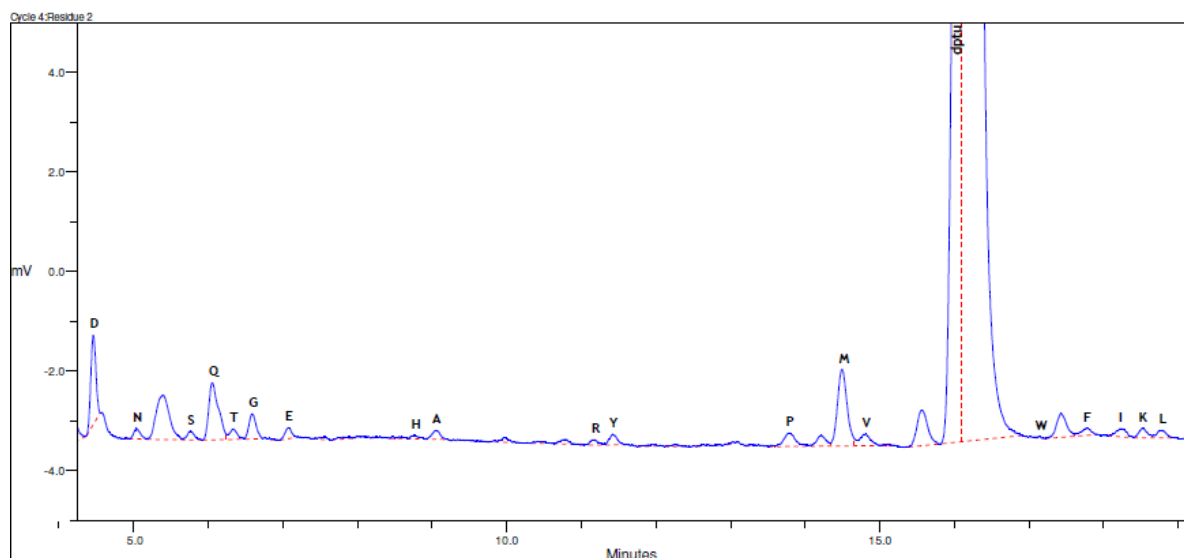
Malihe Masomian, Raja Noor Zaliha Raja Abd Rahman * and Abu Bakar Salleh



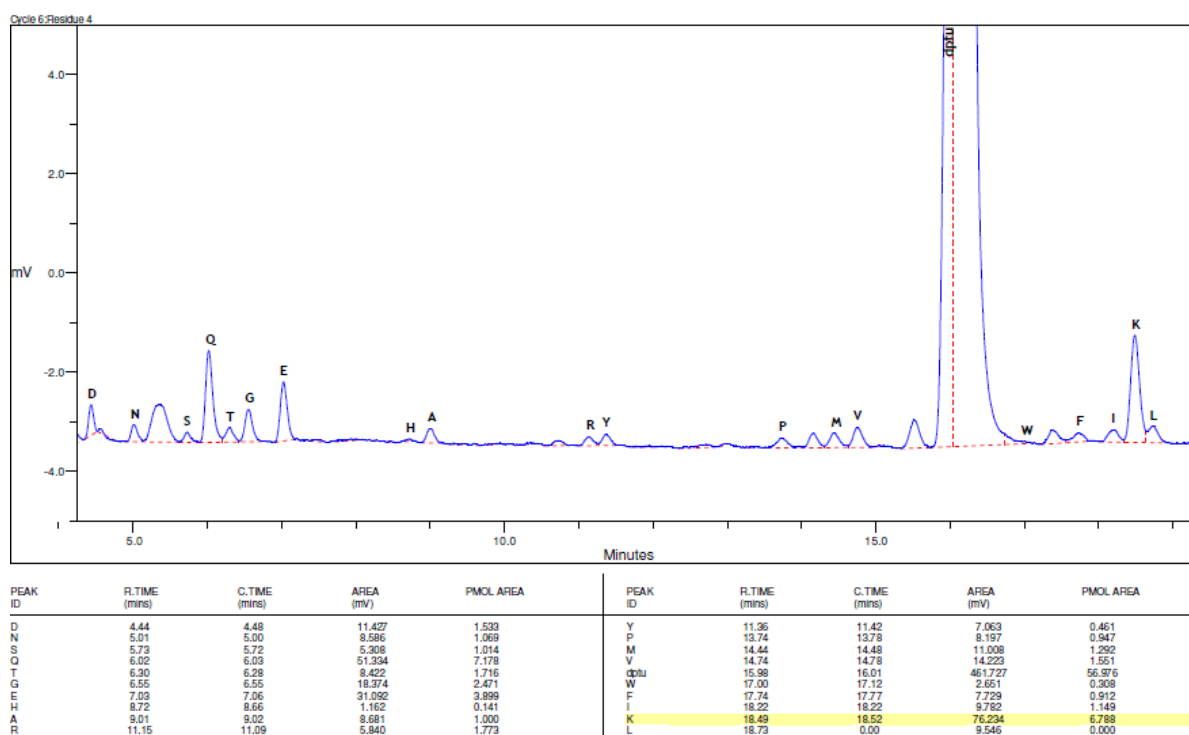
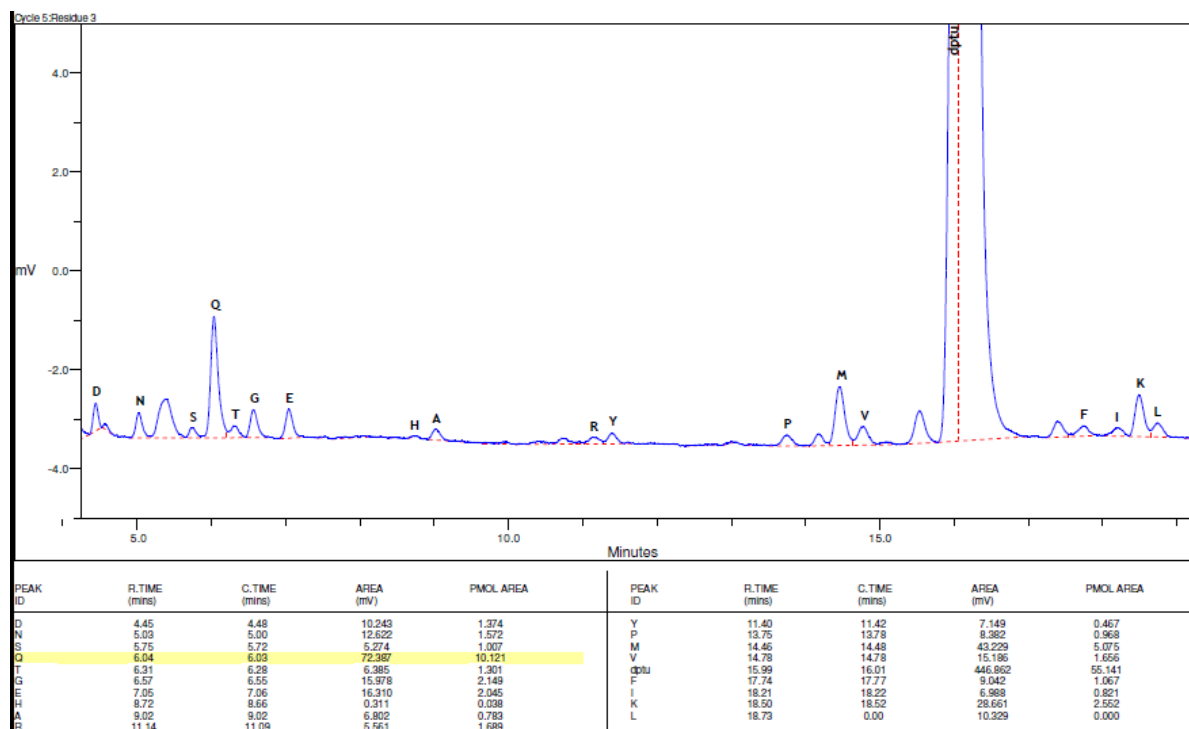
PEAK ID	R.TIME (mins)	C.TIME (mins)	AREA (mV)	PMOL AREA	PEAK ID	R.TIME (mins)	C.TIME (mins)	AREA (mV)	PMOL AREA
D	4.48	4.48	74.544	10.000	Y	11.42	11.42	153.064	10.000
N	5.00	5.00	80.317	10.000	P	13.78	13.78	86.576	10.000
S	5.72	5.72	52.359	10.000	M	14.48	14.48	85.189	10.000
Q	6.03	6.03	71.520	10.000	V	14.78	14.78	91.717	10.000
T	6.28	6.28	49.090	10.000	dptu	16.01	16.01	81.040	10.000
G	6.55	6.55	74.365	10.000	W	17.12	17.12	86.068	10.000
E	7.06	7.06	79.752	10.000	F	17.77	17.77	84.756	10.000
H	8.66	8.66	82.464	10.000	I	18.22	18.22	85.159	10.000
A	9.02	9.02	86.848	10.000	K	18.52	18.52	112.315	10.000
R	11.09	11.09	32.934	10.000					

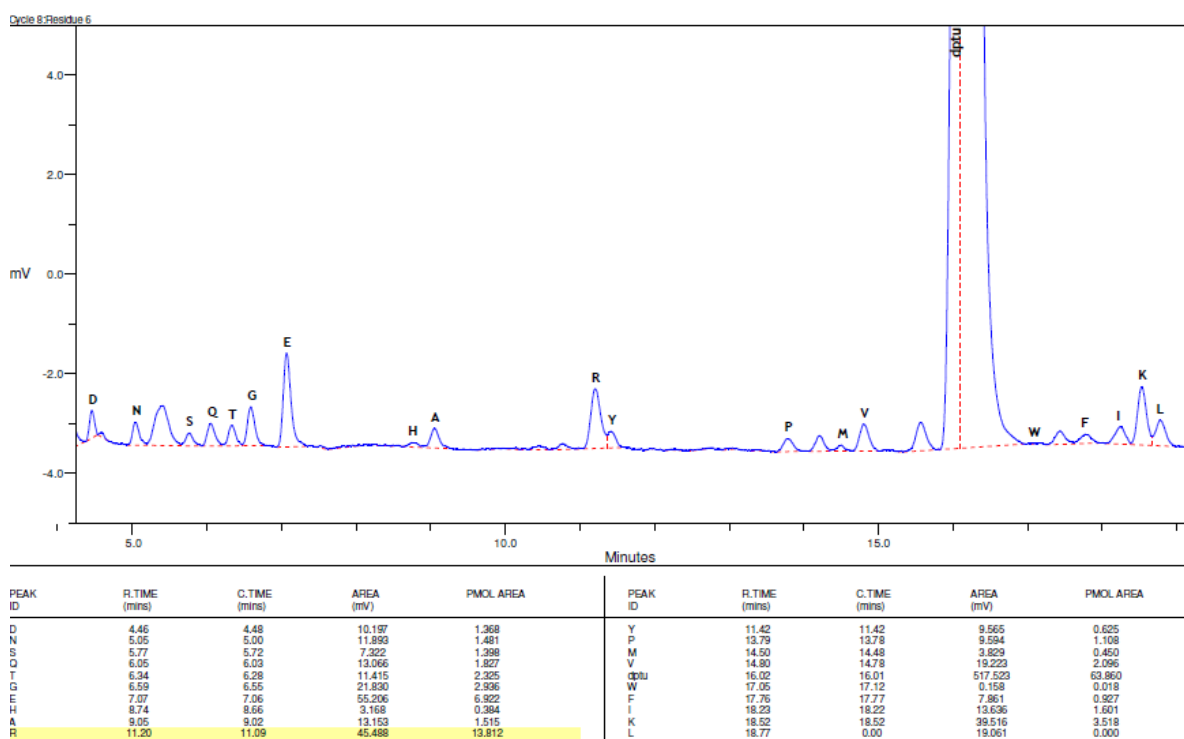
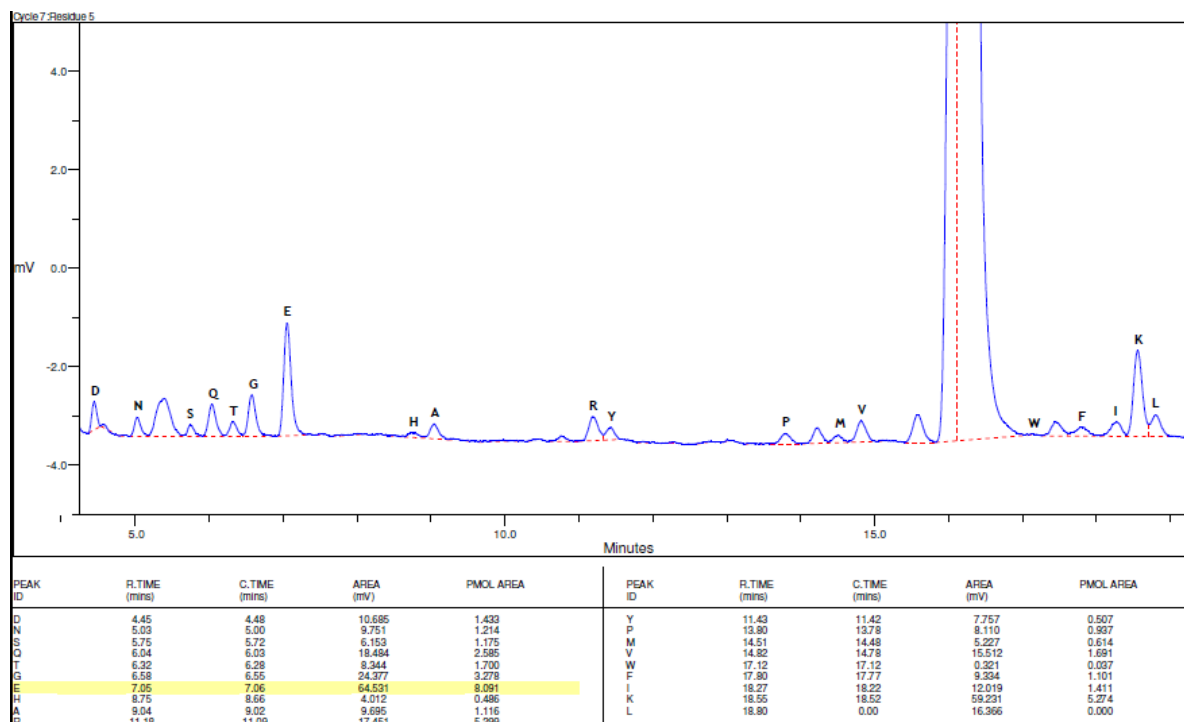


PEAK ID	R.TIME (mins)	C.TIME (mins)	AREA (mV)	PMOL AREA	PEAK ID	R.TIME (mins)	C.TIME (mins)	AREA (mV)	PMOL AREA
D	4.48	4.48	43.929	5.880	Y	11.42	11.42	6.260	0.343
N	5.05	5.00	4.217	0.525	P	13.77	13.78	4.763	0.550
S	5.77	5.72	7.967	1.522	M	14.48	14.48	53.581	6.290
O	6.05	6.03	47.165	6.595	V	14.78	14.78	3.841	0.419
T	6.35	6.28	5.551	1.131	dpbu	16.00	16.01	698.593	86.200
G	6.59	6.55	11.909	1.488	W	17.10	17.12	7.407	0.851
E	7.09	7.06	4.778	0.599	F	17.77	17.77	3.786	0.447
H	8.77	8.66	5.514	0.669	I	18.19	18.22	3.203	0.376
A	9.05	9.02	6.178	0.711	K	18.52	18.52	6.653	0.562
R	11.17	11.09	3.768	1.144	L	18.75	0.00	5.300	0.000



PEAK ID	R.TIME (mins)	C.TIME (mins)	AREA (mV)	PMOL AREA	PEAK ID	R.TIME (mins)	C.TIME (mins)	AREA (mV)	PMOL AREA
D	4.46	4.48	34.173	4.584	Y	11.42	11.42	6.485	0.424
N	5.04	5.00	5.159	0.642	P	13.79	13.78	12.121	1.400
S	5.77	5.72	4.619	0.882	M	14.50	14.48	57.321	6.729
Q	6.05	6.03	42.943	6.004	V	14.91	14.78	7.980	0.859
T	6.33	6.28	4.506	0.918	dpbu	16.02	16.01	488.548	60.285
G	6.59	6.55	19.468	1.811	W	17.13	17.12	0.533	0.062
E	7.08	7.06	5.564	0.598	F	17.77	17.77	5.488	0.548
H	8.77	8.66	2.116	0.257	I	18.25	18.22	6.292	0.751
A	9.05	9.02	5.470	0.630	K	18.52	18.52	5.724	0.510
R	11.18	11.09	3.358	1.020	L	18.78	0.00	5.401	0.000





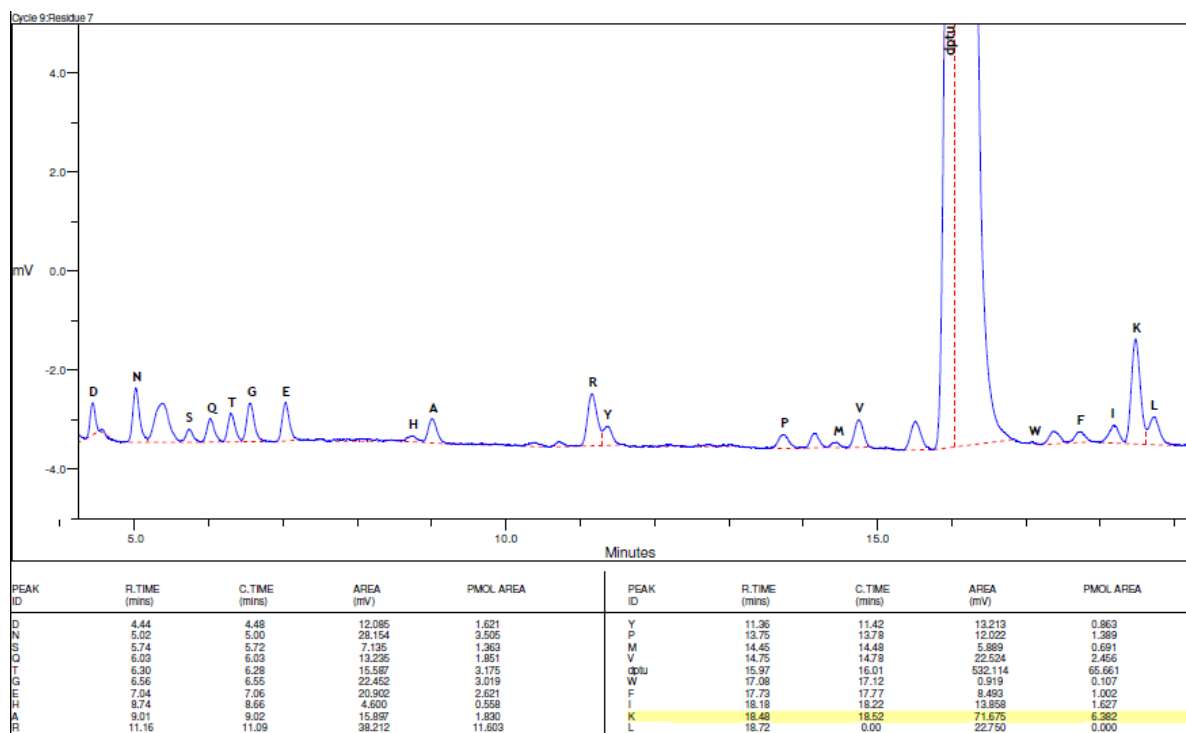
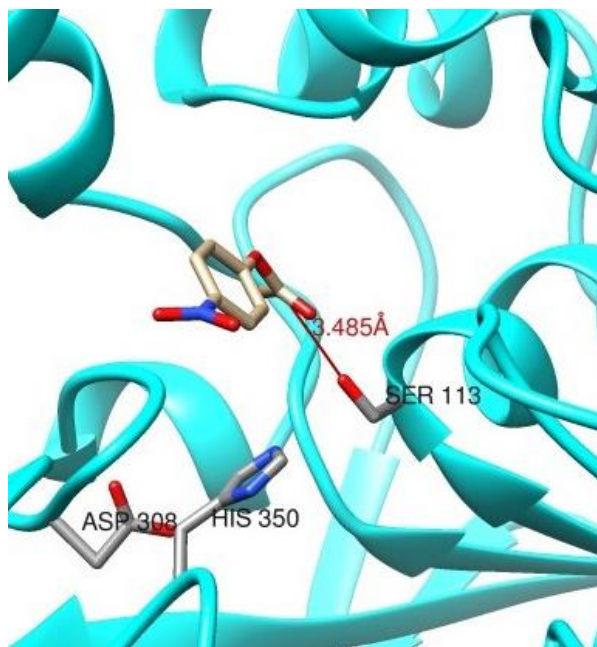


Figure S1. N-terminal sequencing chromatogram.

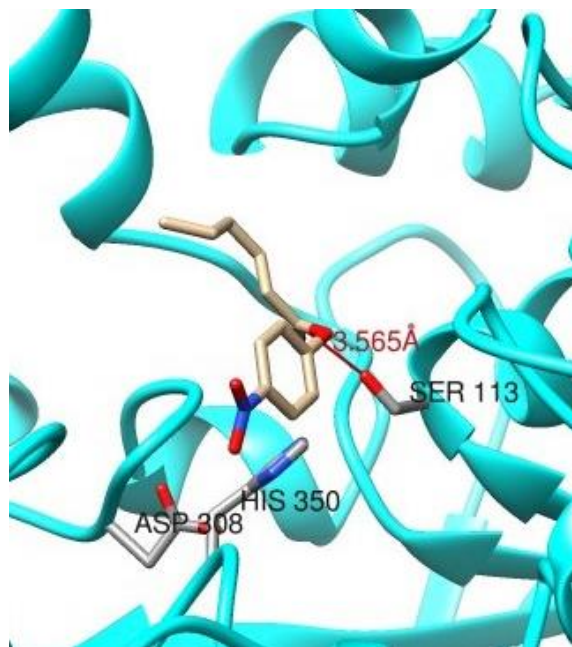
Table S1. Fatty acid composition (%) of edible fats and oils.

Name of the Oil	Caprylic (Octoic) C8	Capric (Decoic) C10	Lauric (Dodecanoic) C12	Myristic (Tetradecanoic) C14	Palmitic (Hexadecanoic) C16	Stearic (n-Octadecanoic) C18	Oleic (C18:1)	Linolenic (C18:3)	Linoleic (C18:2)	Arachidic C20 (Eicosanoic)
Coconut Oil	5.0-9.0	6.0-10.0	44.0-52.0	13.0-19.0	8.0-11.0	1.0-3.0	5.0-8.0	----	0-1.0	0-0.5
Palm Kernal Oil	3.0-5.0	3.0-7.0	40.0-52.0	14.0-18.0	7.0-9.0	1.0-3.0	11.0-19.0	----	0.5-2.0	
Palm Oil	----	----	----	0.5-2.0	32.0-45.0	2.0-7.0	38.0-52.0	----	5.0-11.0	----
Rice Bran Oil	----	----	----	0.4-1.0	12.0-18.0	1.0-3.0	40.0-50.0	0.5-1.0	29.0-42.0	----
Olive Oil	----	----	----	0.1-1.2	7.0-16.0	1.0-3.0	65.0-80.0	----	4.0-10.0	0.1-0.3
Sesame Oil	----	----	----	----	7.0-9.0	4.0-5.0	40.0-50.0	----	35.0-45.0	0.4-1.0
Soya Bean Oil	----	----	----	0.5	7.0-11.0	2.0-6.0	22.0-34.0	5.0-11.0	43.0-56.0	----
Corn Oil	4.0	7.0	----	0.2-1.0	8.0-12.0	2.0-5.0	19.0-49.0	----	34.0-62.0	----
Sunflower Seed Oil	----	----	----	----	3.0-6.0	1.0-3.0	14.0-35.0	----	44.0-75.0	0.6-4.0

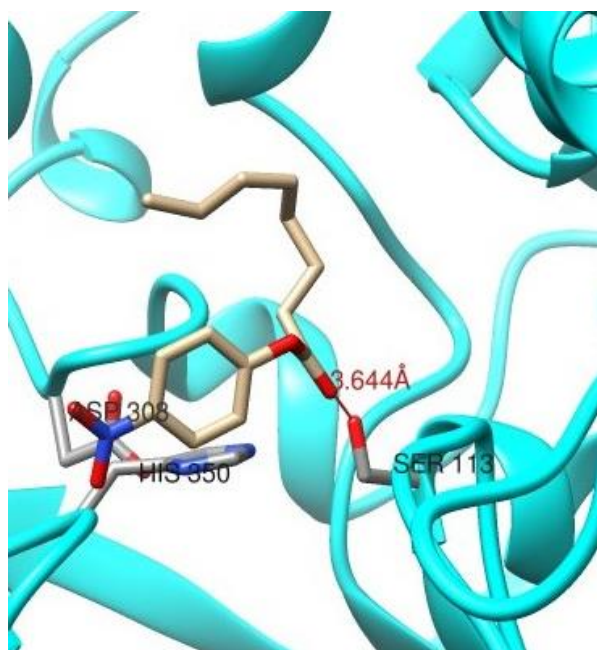
Note: Retrieve from <https://www.chempro.in/fattyacid.htm>.



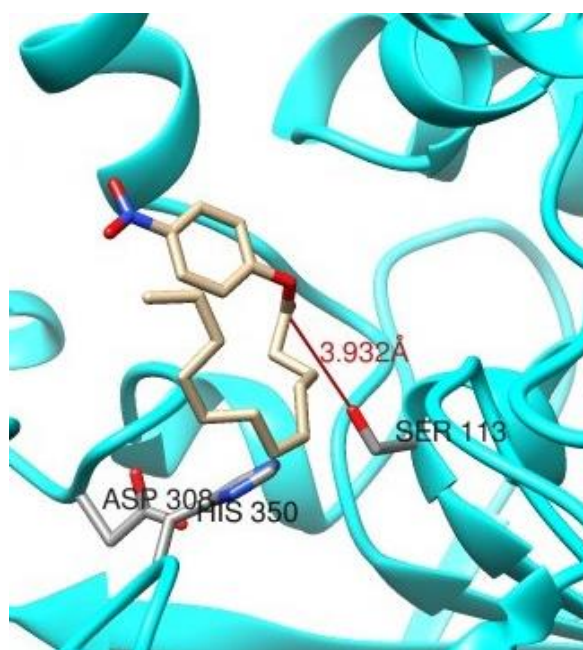
4-nitrophenyl acetate (C2)



4-nitrophenyl hexanoate (C6)



4-Nitrophenyl octanoate (C8)



4-nitrophenyl laurate (C12)

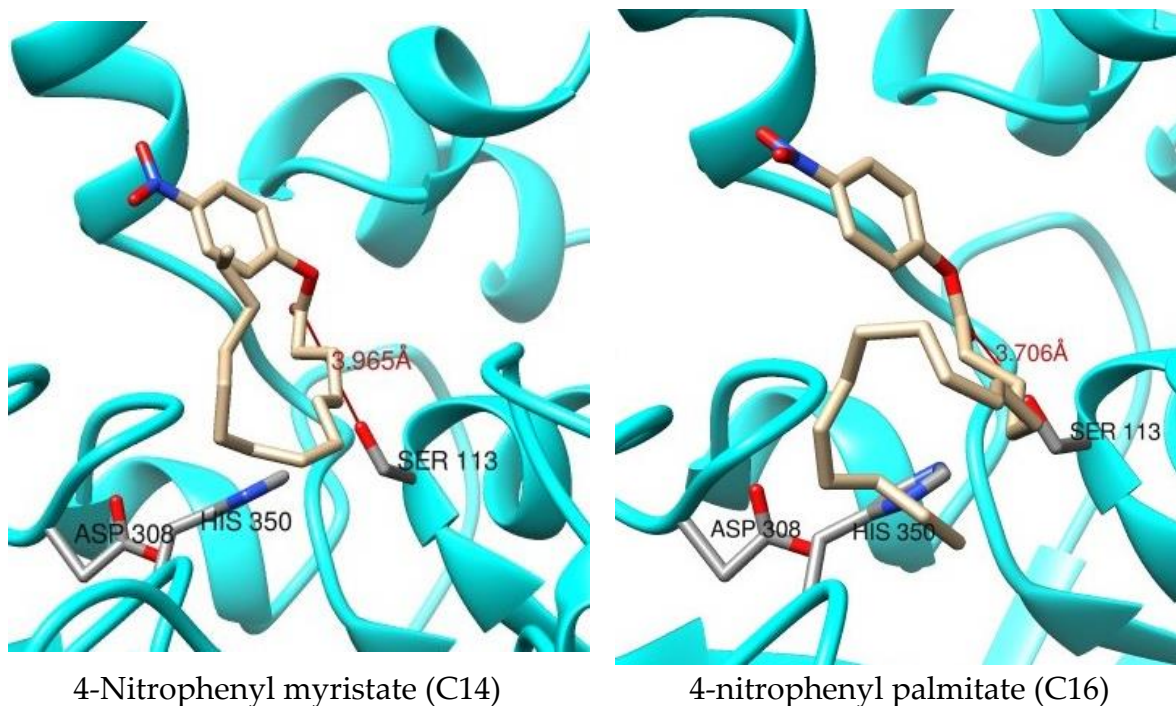


Figure S2. The best binding mode of the complexes between rHZ lipase and 4-nitrophenyl esters with higher binding energy and lower distance between hydroxyl (O_{γ} -Ser113) and the carbonyl carbon of the substrate.

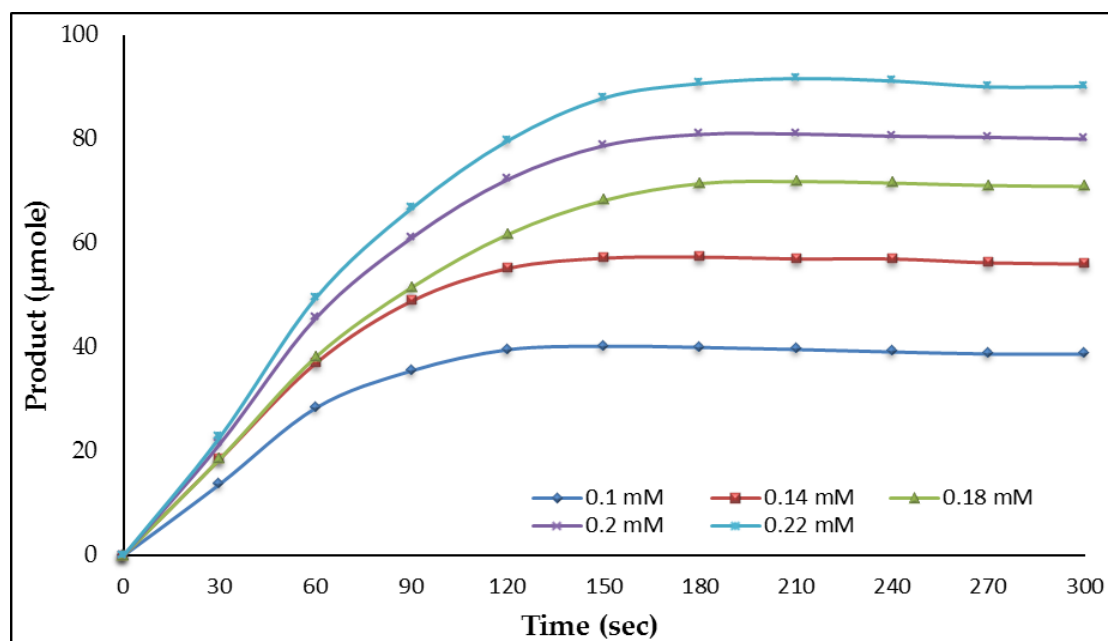


Figure S3. Progress curve of product formed against time.

Table S2. Biochemical properties of *Bacillus* and *Geobacillus* lipases from subfamilies I.4 and I.5.

Subfamily	Lipase origin, Activity test	Molecular weight (kDa)	pH optimum and stability	T optimum and stability	Selectivity	Solvents	Surfactant, Inhibitors	Metal ions	Reference
I.4	<i>Bacillus subtilis</i> LipB	19.5	10	35–40 °C	TAGs: C8:0 > C6 > C4 > C10 > C3 > C2 > C12 pNP esters: C8 > C14:0 > C12:0 > C10, C6 > C18:0 > C4				[1]
I.4	<i>Bacillus subtilis</i> 168 LipA Hydrolysis of tributyrin	19	10 24 h, pH = 13 (65%)	35 °C 30 min, T = 55 °C (0%)	pNP esters: C8 > C12 > C4 > C16, C18 TAGs: C8 >> C4 > C16 > C12 > C2 C18 (0%)	60% (v/v) DMSO (0%); 30% (v/v) DMSO (140%); i-propanol (0%); acetone (0%); ethanol; pyridine	0.1mM PMSF (30%) 1mM PMSF (0%)	10 mM Ca ²⁺ (294%); Cu ²⁺ (45%); Mn ²⁺ (32%); Zn ²⁺ (37%)	[2]
I.4	<i>Bacillus pumilus</i> B26 Hydrolysis of olive oil	19.2	8.5	35 °C	TAGs: C3 > C4 > C6 > C2 > C8 > C10 > C16, C14, C18		5 mM EDTA (100%)	10 mM Ca ²⁺ (100%)	[3]
I.4	<i>Bacillus pumilus</i> B106 Hydrolysis of pNP acetate		8.0 1 h, pH = 7.0–9.0 (>65%)	50 °C 1 h, T = 30–50 °C (>55%)		10% (v/v) methanol (138%); 20% (v/v) methanol (127%); 10% (v/v) DMSO (91%); ethanol (88%); i-propanol (81%); 30% (v/v) methanol (63%)			[4]

I.5	<i>Bacillus</i> sp. strain 42 Hydrolysis of olive oil	43	8.0 7–10	70 °C $\tau_{1/2}$ (60 °C) = 5 h 15 min $\tau_{1/2}$ (65 °C) = 2 h 5 min $\tau_{1/2}$ (70 °C) = 45 min	25% (v/v) benzene (105%); n-hexane (104%); n-hexadecane (104%); tetradecane (94.5%); i-octane (93.4%); decanol (90%); toluene (84.7%); p-xylene (79.7%); dodecanol (71%); propyl acetate (63.6%); ethyl acetate (46.4%); 1-propanol (34.5%)	[5,6]	
I.5	<i>Bacillus</i> sp. L2 Hydrolysis of olive oil	45	8.0	70 °C $\tau_{1/2}$ (60 °C) = 3.5 h $\tau_{1/2}$ (65 °C) = 106 min	TAGs: C16 > C12 > C14, C10 > C18:1 > C18:0 > C8 > C6 > C4 > C2 Natural oils	1 mM 2-mercaptoethanol (98.6%); DTT (77.5%); PMSF (8.7%); pepstatin A (3.2%); EDTA (0.4%) 10 mM Ca ²⁺ (510%); 1 mM Ca ²⁺ (395%); Na ⁺ (301%); Cu ²⁺ (222%); Mn ²⁺ (209%); Fe ³⁺ (114%); K ⁺ (100%); Zn ²⁺ (61%); Mg ²⁺ (26%); K ⁺ (53); Fe ³⁺ (33%); Mn ²⁺ (31%); Cu ²⁺ (0%)	[7]

I.5	<i>Geobacillus zalihae</i> T1 Hydrolysis of olive oil	43.0	9.0	70 °C 30 min, pH = 9.0–11.0, T = 50 °C (>60%)	$\tau_{1/2}$ (65 °C) = 5h 15 min; $\tau_{1/2}$ (70 °C) = 70min	TAGs: C12 > C14 > C10 > C16 > C8 > C18:1 > C6 > C18 > C4 > C2 Natural oils	1 mM Tween 20 (122%); Tween 40 (101%); Tween 60 (126%); Tween 80 (188%); Triton X-100 (72%); SLS (48%); SDS (5%) 5 mM PMSF (11%) 1 mM pepstatin (14%)	1 mM Ca ²⁺ (100%); Na ⁺ (99%); Mn ²⁺ (87%); K ⁺ (81%); Mg ²⁺ (81%); Cu ²⁺ (49%); Fe ³⁺ (39%); Zn ²⁺ (22%)	[8,9]
I.5	<i>Geobacillus stearothermophilus</i> P1 Hydrolysis of pNP caprate, olive oil	43.2	8.5	55 °C $\tau_{1/2}$ (55 °C) = 7.6 h	pNP esters: C10 > C8 > C12 > C14 > C16:0 > C18:0, C6 > C4 TAGs: C8 > C10 > C12 > C14 > C6 > C16:1 > C18:3, C16:0 > C18:1 > C18:2 > C18:0, C20:1 > C4, C10:0 > C22, C22:0	1 h incubation with 1% (w/v) CHAPS (58%); Triton X-100 (50%); sodium deoxycholate (42%); SDS (37%); Tween 20 (14%) 30 min incubation with 10 mM β -mercaptoethanol (80%); DTT (74%); EDTA (69%); PMSF (2%); 1-dodecanesulfonyl chloride (5%); 1-hexadecane-sulfonyl chloride (0%)	10 mM Ca ²⁺ (92%); Na ⁺ (90%); Mg ²⁺ (90%); Cs ⁺ (84%); K ⁺ (72%); Li ⁺ (71%); Cu ²⁺ (63%); Mn ²⁺ (41%); Zn ²⁺ (1.6%); Fe ²⁺ (0.76%)	[10,11]	
I.5	<i>Geobacillus thermoleovorans</i> ID-1 LipB Hydrolysis of tricaprylin	43	8.0–9.0	60 °C $\tau_{1/2}$ (70 °C) = 30min	TAGs: C10, C8, C16 > C12 > C6 > C14 > C18 > C4	1% (v/v) i-propanol (130%); DMSO (126%); ethanol (124%)	1% (w/v) 2-mercaptoethanol (135%); DTT (129%); PMSF (124%); EDTA (55%)	1 mM Na ⁺ (124%); Mn ²⁺ (124%); K ⁺ (120%); Ca ²⁺ (121%); Co ²⁺ (119%); Ag ⁺ (109%); Hg ²⁺ (87%); Fe ²⁺ (64%); Zn ²⁺ (63%); Cu ²⁺ (56%)	[12]

I.5	<i>Geobacillus thermocatenulatus</i> BTL2 Hydrolysis of olive oil, pNP palmitate, tributyrin	43	8.0–9.0 12 h, T = 30°C, pH = 9.0–11.0 (90–100%)	60–70 °C 30 min, pH 9.0, T = 30–50 °C (>80%)	pH 7.5 TAGs: C4 > C6 > C8 > C10 > C12 > C16, C18 > C2 > C14 pNP esters: C10 > C12 > C14 > C16 >C8>C6>C2>C4 pH 8.5 TAGs: C4 > C18 >C16>C12>C8 pNP esters: C8 > C10 > C12 > C14 > C16 > C18 >C6>C3>C4, C2 TAGs: C3 > C4 > C12 > C14, C16 > C6, C10 > C8 > C18:1, C18:3 > C18:2 > C18:0 > C2	0 min incubation 30% (v/v) methanol (118%); ethanol (100%); acetone (100%); i-propanol (100%) 30 min incubation 30% (v/v) i-propanol (95%); ethanol (90%); acetone (82%); methanol (80%)	0 min incubation 0.1% lubrol PX (139%); Tween 20 (137%); Triton X-100 (119%) 1% (w/v) CHAPS (184%); octylglucoside (180%); Brij 35 (163%); Triton X-100 (0%); Tween 80 (0%) No effect: 10 mM EDTA; 1mM NaN ₃ ; PMSF 1mM PMSF (90%); EDTA (89%); iodoacetamide (85%); E600 (71%) 1% (v/v) 2-mercaptoethanol (89%); sodium deoxycholate (83%); Triton X-100 (83%); SDS (2%)	10mM Ca ²⁺ ; Mg ²⁺ (100%); Mn ²⁺ (69%); 1m MAg ⁺ (72%)	[13]
I.5	<i>Geobacillus stearothermophilus</i> L1 Hydrolysis of olive oil	43	9.0–10.0 Stable 24 h, pH = 5.0–11.0	60 °C 30 min, T = 30–60 °C (>80%)				1 mM Ca ²⁺ (100%); Mg ²⁺ (90%); Mn ²⁺ (89%); Zn ²⁺ (85%); Fe ²⁺ (81%); Hg ²⁺ (25%); Cu ²⁺ (13%)	[4,14]

Note: Values in brackets represent residual lipolytic activity.

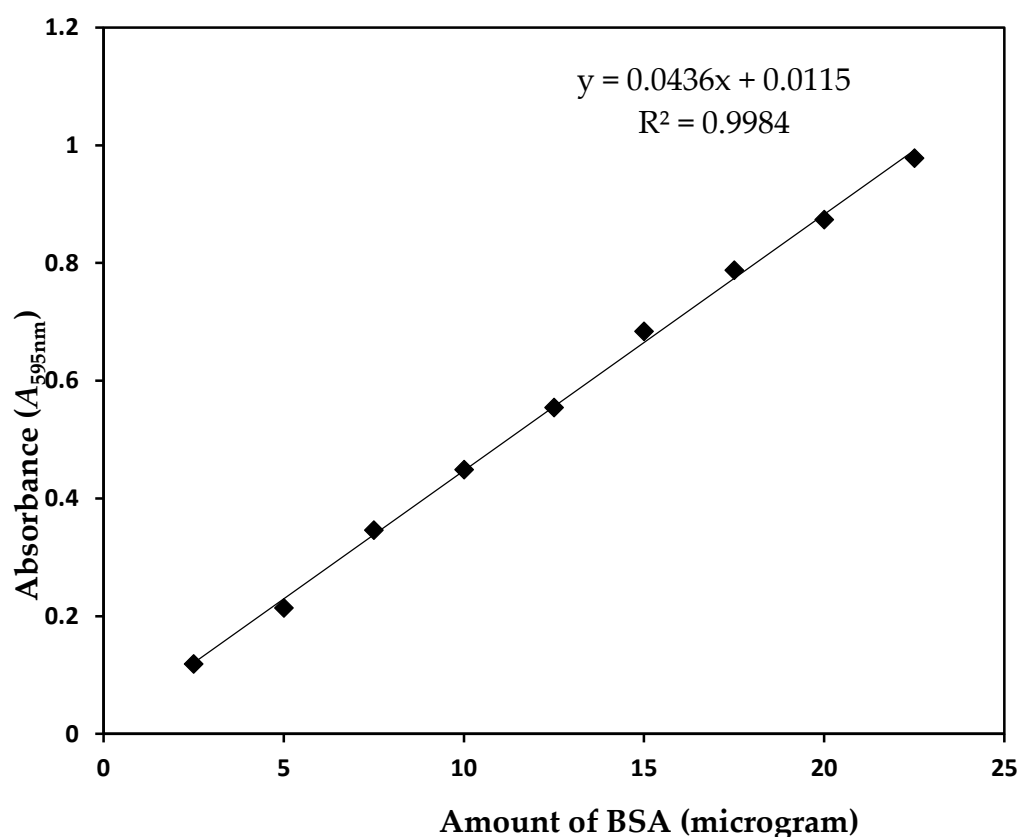


Figure S4. Calibration curve for determination of protein content by Bradford assay.

Text S1: The rHZ lipase structure prediction in Open conformation.

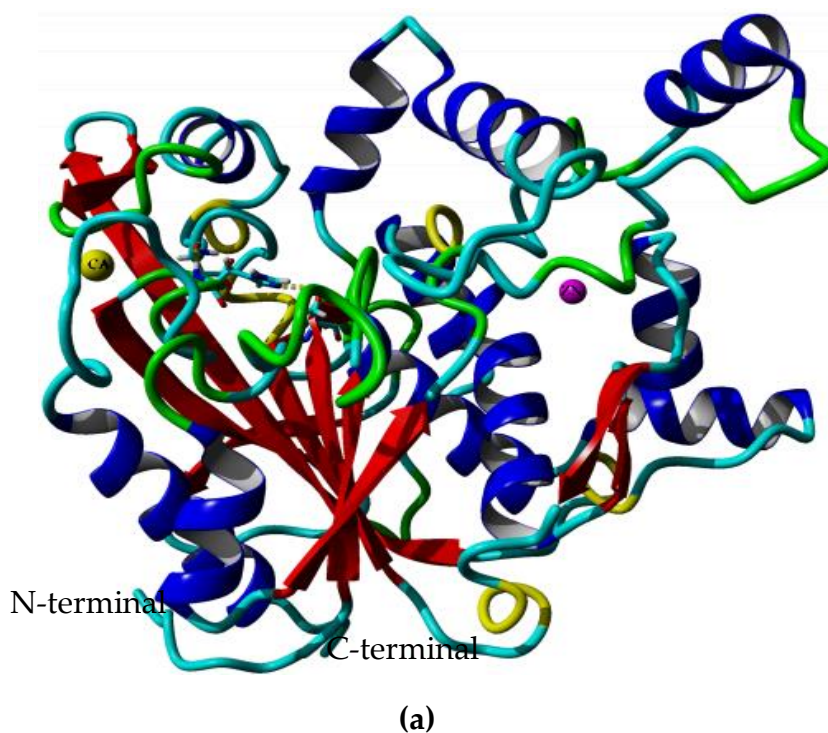
In the first attempt, molecular docking study was performed using the closed conformation of predicted structure of rHZ lipase. The analysis of result showed the long distance between hydroxyl (O γ -Ser113) and the carbonyl carbon of the substrate which indicated the impossibility of hydrolysis reaction process. The rHZ lipase has a large lid domain contained two helices that cover the active site. Hence, for molecular docking study, the structure of enzyme was predicated in an open conformation. Carrasco-Lopez et al. [15] showed that thermostable BTL2 lipase activation involved large structural rearrangements of around 70 amino acids and the concerted movement of two lids, the α 6- and α 7-helices, unmasking the active site. Based on the result of PSI-Blast, the rHZ lipase showed high identity with the crystal structure of thermostable BTL2 lipase from subfamily I.5 (PDB ID: 2W22) with sequence identities of 56% (Table S3). As the model was built by the YASARA and SWISS-MODEL program, the crystal structure of thermostable lipase from the same family of the enzyme with similar function was chosen as the templates to extrapolate structure information of the rHZ lipase [16]. YASARA Structure involves a complete homology modeling module that fully and automatically takes all the steps from an amino acid sequence to a refined reliable model using a CASP (Critical Assessment of protein Structure Prediction) approved protocol [17]. SWISS-MODEL is a web-based integrated service which performs the alignment of the target sequence and template structure(s), model-building, and model quality evaluation. These steps would be done by specialized software and integrate up-to-date protein sequence and structure databases. Each of the above steps would be repeated interactively until a satisfying modeling result is achieved.

Table S3. PSI blast of HZ lipase gene from *A. thermoaerophilus* strain HZ with lipases with open conformation.

Crystal structure	Subfamily	Length	E_value	Identity (%)	Resolution (Å)
>gi 218681560 pdb 2W22 A	I.5	389	3e-132	56	2.2
>gi 149241972 pdb 2HIH A	I.6	431	3e-83	40	2.86
>gi 11514465 pdb 1EX9 A	I.1	285	4e-06	24	2.54

Note: *Bacillus thermocatenulatus* BTL2 lipase (2W22), *Staphylococcus hyicus* lipase (2HIH) and *Pseudomonas aeruginosa* lipase (1EX9).

The predicted model of rHZ lipase with an open conformation by both software contained one main region. However, YASARA predicted model consisted of 11 α -helices and 10 β -sheets and SWISS-MODEL predicted structure consisted of 11 α -helices and 11 β -sheets in the folded protein (Figure S5). The β -sheets were in the core region surrounded by α -helices to form a typical α/β hydrolase. Three catalytic residues include Ser113, His308, and Asp350. YASARA predicted two metal ions, Zn²⁺ and Ca²⁺, in rHZ lipase structure which is common in all crystal structures of thermostable lipases in subfamily I.5 while, SWISS-MODEL predicted structure was contained only Zn²⁺.



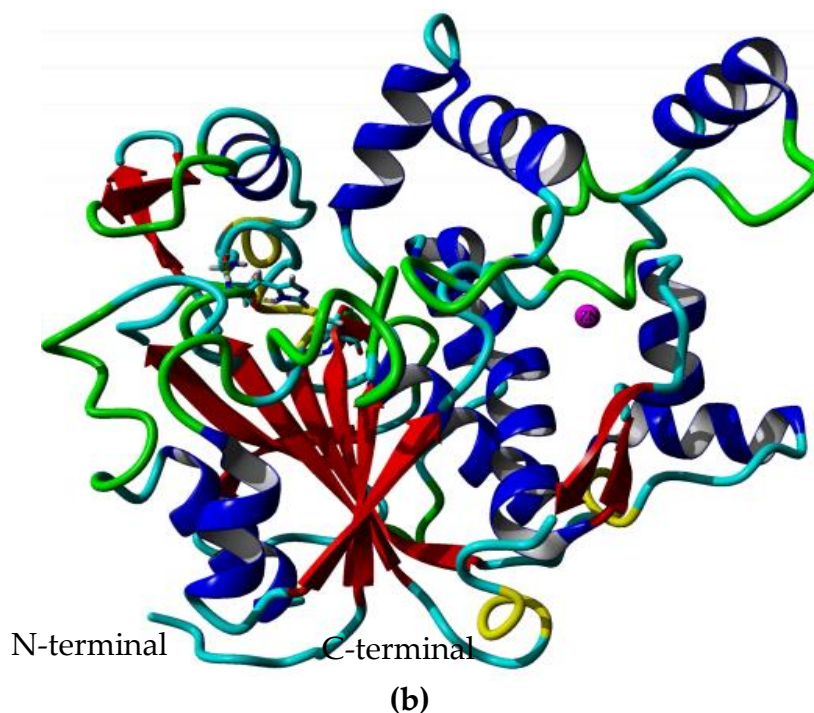
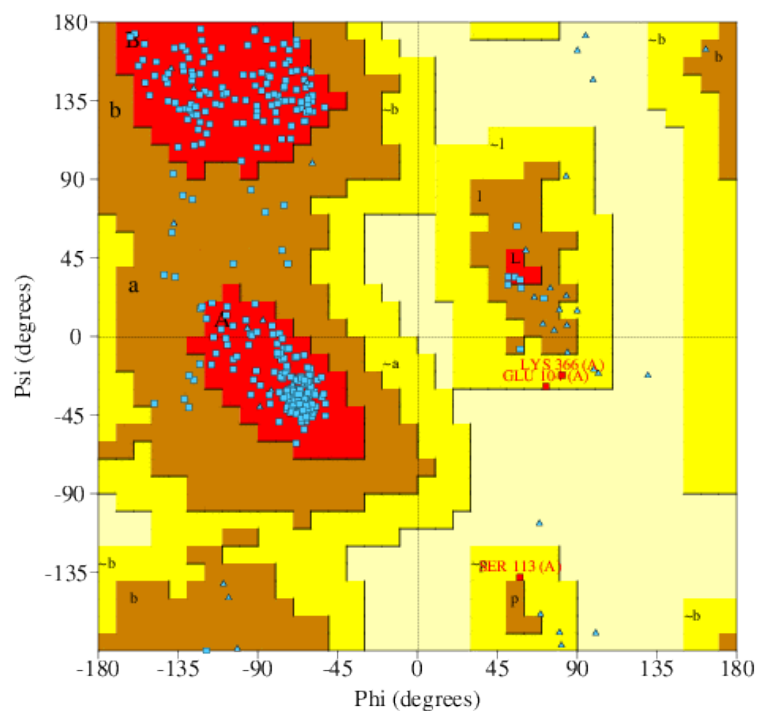
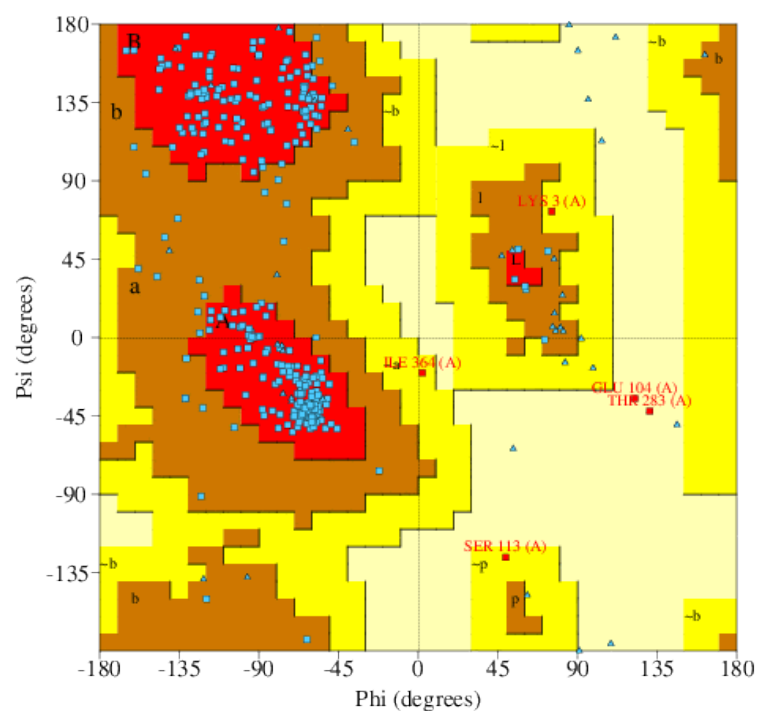


Figure S5. Predicted 3D structure of rHZ lipase using the 3D structure of 2W22 (BTL2 lipase) by (a) YASARA and (b) SWISS-MODEL in the linear ribbon. Metal ions, Ca^{2+} and Zn^{2+} are shown as solid circles. α -helices (blue), β -sheets (red), turn (yellow) and 310-helix (green) are arranged in a single domain.

The validity of the structures was confirmed by three different software. Favored regions of Ramachandran plot are energetically and sterically stable conformations of residues characterized by values of torsion angles ψ and ϕ . The Ramachandran plot of the predicted rHZ lipase structure by YASARA revealed that 91.0% (295) of the residues lie in the most-favored region, with 8.0% (26) of residues in the additional allowed region and 0.9% (3) of residues in generously allowed regions (Figure S6). While, the Ramachandran plot of the predicted structure by SWISS-MODEL showed that 87.2% (279) of the residues lie in the most-favored region, with 11.2% (36) of residues in the additional allowed region and 0.9% (3) of residues in generously allowed regions and 0.6% (2) of residues lie in disallowed regions (Figure S6). For both models, the compatibility of segments of the rHZ lipase amino acid sequence with their 3D structure of rHZ lipase was assessed by plotting the 3D-1D averaged score against sequence number. In the YASARA predicted structure, the 3D-1D averaged score fluctuated from -0.09 to 0.68, 85.94.9% of the total residues of the predicted model have 3D-1D averaged score of ≥ 0.2 , while, in the predicted rHZ lipase structure by SWISS-MODEL, the 3D-1D averaged score fluctuated from -0.02 to 0.68, 84.74.9% of the total residues of the predicted model have 3D-1D averaged score of ≥ 0.2 (Figure S7). Based on the analysis by ERRAT, the predicted model by YASARA was significantly acceptable according to 98.13% overall quality factor, while the predicted model by SWISS-MODEL showed 94.89% overall quality factor (Figure S8).

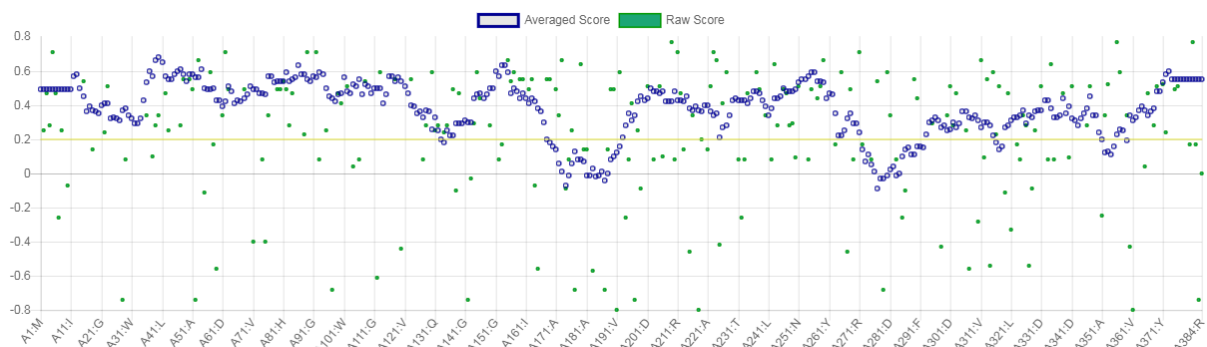


(a)

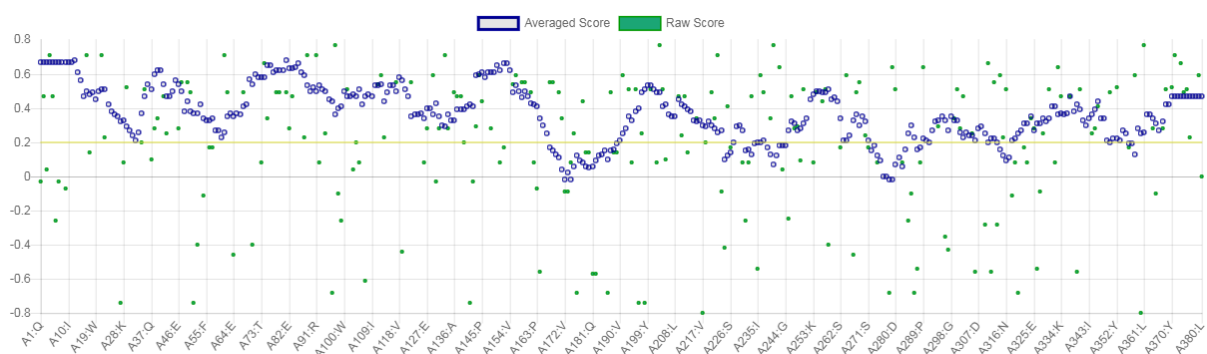


(b)

Figure S6. Ramachandran plot of predicted rHZ lipase structures modeled by (a) SWISS-MODEL and (b) YASARA. The most favored region (red), additional allowed region (orange-brown), generously allowed region (dark yellow) and disallowed region (light yellow) were used to evaluate the quality of the structure. Note: Based on an analysis of 118 structures of resolution of at least 2.0 Angstroms and *R*-factor no greater than 20.0 a good quality model would be expected to have over 90% in the most favored regions [A, B, L].



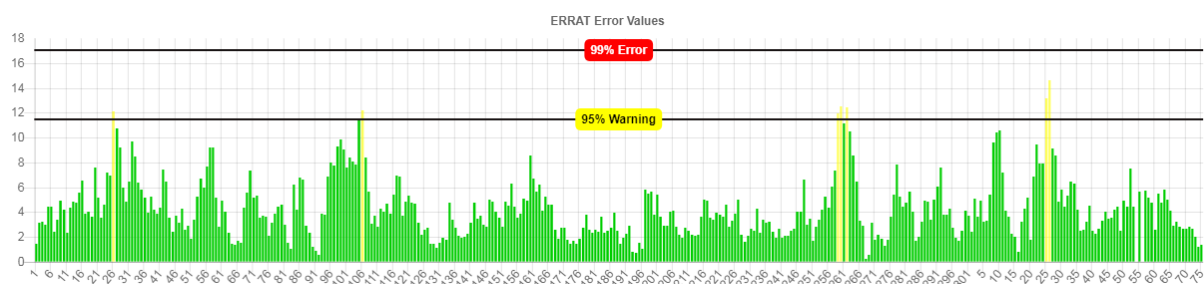
(a) Modeled by YASARA



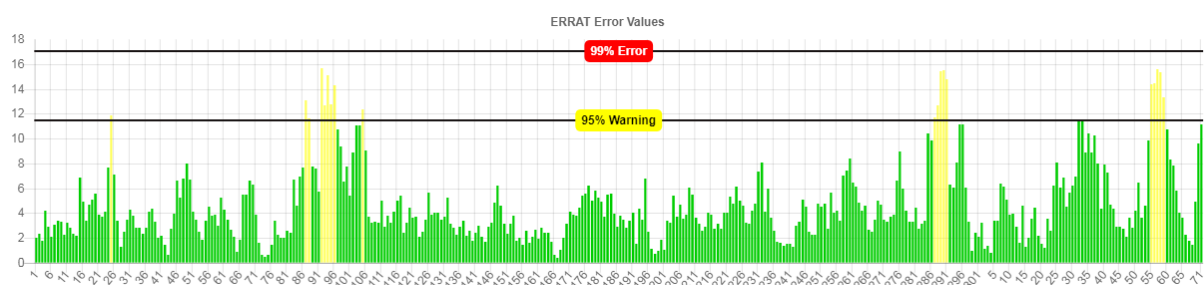
(b) Modeled by SWISS-MODEL

Note: At least 80% of the amino acids have scored ≥ 0.2 in the 3D/1D profile.

Figure S7. Verify 3D structure evaluation of HZ lipase modeled by (a) YASARA and (b) SWISS-MODEL.



(a) Modeled by YASARA



(b) Modeled by SWISS-MODEL

Figure S8. Evaluation of predicted HZ lipase structure modeled by (a) YASARA and (b) SWISS-MODEL with ERRAT.

The summary of the evaluation showed that the structure predicted by YASARA is more reliable compared to the structure predicted by SWISS-MODEL (Table S4). Hence, the predicted structure by YASARA was selected for the molecular docking study.

Table S4. Summary of evaluation of two predicted rHZ lipase structures.

Program	Ramachandran Plot statistics (http://www.ebi.ac.uk/thornton-srv/databases/pdbsum/Generate.html)	Verify3D (http://servicesn.mbi.ucla.edu/Verify3D/)	ERRAT (http://servicesn.mbi.ucla.edu/ERRAT/)	
rHZ lipase Model				
	residues	%-tage		
YASARA	Most favored regions	295	91.0%	
	Additional allowed regions	26	8.0%	
	Generously allowed regions		85.94%	98.13
	Disallowed regions	3	0.9%	
SWISS-MODEL		0	0.0%	
	Most favored regions	279	87.2%*	
	Additional allowed regions	36	11.2%	
	Generously allowed regions		84.74%	94.89
	Disallowed regions	3	0.9%	
		2	0.6%*	

References

1. Eggert, T.; van Pouderoyen, G.; Pencreac'h, G.; Douchet, I.; Verger, R.; Dijkstra, B.W.; Jaeger, K.-E. Biochemical properties and three-dimensional structures of two extracellular lipolytic enzymes from *Bacillus subtilis*. *Colloids Surf. B: Biointerfaces* **2002**, *26*, 37–46.
2. Lesuisse, E.; Schanck, K.; Colson, C. Purification and preliminary characterization of the extracellular lipase of *Bacillus subtilis* 168, an extremely basic pH-tolerant enzyme. *Eur. J. Biochem.* **1993**, *216*, 155–160.
3. Kim, H.K.; Choi, H.J.; Kim, M.H.; Sohn, C.B.; Oh, T.K. Expression and characterization of Ca²⁺-independent lipase from *Bacillus pumilus* B26. *Biochim. Biophys. Acta (BBA) - Mol. Cell Biol. Lipids* **2002**, *1583*, 205–212.
4. Genckal, H.; Tari, C. Alkaline protease production from alkalophilic *Bacillus* sp. isolated from natural habitats. *Enzym. Microb. Technol.* **2006**, *39*, 703–710.
5. Rahman, R.N.Z.R.A.; Hamid, T.H.T.A.; Eltaweel, M.A.; Basri, M.; Salleh, A.B. Overexpression and characterization of strep-tagged thermostable organic solvent-stable lipase from *Bacillus* sp. strain 42. *J. Biotechnol.* **2008**, *136*, 335S.
6. Eltaweel, M.A.; Rahman, R.N.Z.R.A.; Salleh, A.B.; Basri, M. An organic solvent-stable lipase from *Bacillus* sp. strain 42. *Ann. Microbiol.* **2005**, *55*, 187–192.
7. Sabri, S.; Rahman, R.N.Z.R.A.; Leow, T.C.; Basri, M.; Salleh, A.B. Secretory expression and characterization of a highly Ca²⁺-activated thermostable L2 lipase. *Protein Expr. Purif.* **2009**, *68*, 161–166.
8. Leow, T.C.; Rahman, R.N.Z.R.A.; Basri, M.; Salleh, A.B. A thermoalkaliphilic lipase of *Geobacillus* sp. T1. *Extremophiles* **2007**, *11*, 527–535.
9. Leow, T.C.; Rahman, R.N.Z.R.A.; Basri, M.; Salleh, A.B. High level expression of thermostable lipase from *Geobacillus* sp. Strain T1. *Biosci. Biotechnol. Biochem.* **2004**, *68*, 96–103.
10. Sinchaikul, S.; Tyndall, J.D.A.; Fothergill-Gilmore, L.A.; Taylor, P.; Phutrakul, S.; Chen, S.T.; Walkinshaw, M.D. Expression, purification, crystallization and preliminary crystallographic analysis of a thermostable lipase from *Bacillus stearothermophilus* P1. *Acta Crystallogr. D Biol. Crystallogr.* **2002**, *58*, 182–185.
11. Sinchaikul, S.; Sookkheo, B.; Phutrakul, S.; Pan, F.-M.; Chen, S.-T. Optimization of a thermostable lipase from *Bacillus stearothermophilus* P1: Overexpression, purification, and characterization. *Protein Expr. Purif.* **2001**, *22*, 388–398.
12. Lee, D.-W.; Kim, H.-W.; Lee, K.-W.; Kim, B.-C.; Choe, E.-A.; Seung Lee, H.-; Kim, D.-S.; Pyun, Y.-R. Purification and characterization of two distinct thermostable lipases from the gram-positive thermophilic bacterium *Bacillus thermoleovorans* ID-1. *Enzym. Microb. Technol.* **2001**, *29*, 363–371.
13. Schmidt-Dannert, C.; Rúa, M.L.; Atomi, H.; Schmid, R.D. Thermoalkaliphilic lipase of *Bacillus thermocatenuatus*. I. Molecular cloning, nucleotide sequence, purification and some properties. *Biochim. Biophys. Acta (BBA) - Lipids Lipid Metabolism* **1996**, *1301*, 105–114.
14. Kim, M.-H.; Kim, H.-K.; Lee, J.-K.; Park, S.-Y.; Oh, T.-K. Thermostable lipase of *Bacillus stearothermophilus*: High-level production, purification, and calcium-dependent thermostability. *Biosci. Biotechnol. Biochem.* **2000**, *64*, 280–286.
15. Carrasco-Lopez, C.; Godoy, C.; de las Rivas, B.; Fernandez-Lorente, G.; Palomo, J.M.; Guisan, J.M.; Fernandez-Lafuente, R.; Martinez-Ripoll, M.; Hermoso, J.A. Activation of bacterial thermoalkaliphilic lipases is spurred by dramatic structural rearrangements. *J. Biological Chem.* **2008**, *284*, 4365–4372.
16. Zaki, M.J.; Bystroff, C. *Protein structure prediction*. second ed.; Humana Press Inc.: New York, 2008, ISBN 9781588297525.
17. Krieger, E.; Joo, K.; Lee, J.; Lee, J.; Raman, S.; Thompson, J.; Tyka, M.; Baker, D.; Karplus, K. Improving physical realism, stereochemistry, and side-chain accuracy in homology modeling: four approaches that performed well in CASP8. *Proteins: Struct. Funct. Bioinformatics* **2009**, *77*, 114–122